



## OPEN

# Chromatin compaction under mixed salt conditions: Opposite effects of sodium and potassium ions on nucleosome array folding

## SUBJECT AREAS:

SUPRAMOLECULAR  
ASSEMBLY

BIOLOGICAL MODELS

BIOPHYSICS

Abdollah Allahverdi\*, Qinming Chen, Nikolay Korolev &amp; Lars Nordenskiöld

Received  
17 October 2014Accepted  
7 January 2015Published  
17 February 2015

School of Biological Sciences, Nanyang Technological University, Singapore 637551.

Correspondence and requests for materials should be addressed to N.K. (Korolev@ntu.edu.sg) or L.N. (LarsNor@ntu.edu.sg)

\* Current address: Department of Physics, National University of Singapore, Singapore 117542

It is well known that chromatin structure is highly sensitive to the ionic environment. However, the combined effects of a physiologically relevant mixed ionic environment of  $K^+$ ,  $Mg^{2+}$  and  $Na^+$ , which are the main cations of the cell cytoplasm, has not been systematically investigated. We studied folding and self-association (aggregation) of recombinant 12-mer nucleosome arrays with 177 bp DNA repeat length in solutions of mixtures of  $K^+$  and  $Mg^{2+}$  or  $Na^+$  and  $Mg^{2+}$ . In the presence of  $Mg^{2+}$ , the addition of sodium ions promotes folding of array into 30-nm fibres, whereas in mixtures of  $K^+$  and  $Mg^{2+}$ , potassium ions abrogate folding. We found that self-association of nucleosome arrays in mixed salt solutions is synergistically promoted by  $Mg^{2+}$  and monovalent ions, with sodium being slightly more efficient than potassium in amplifying the self-association. The results highlight the importance of a mixed ionic environment for the compaction of chromatin under physiological conditions and demonstrate the complicated nature of the various factors that determine and regulate chromatin compaction *in vivo*.

To fulfil the requirements of DNA fitting in the limited volume of the cell nucleus without losing its dynamic accessibility for transcription, replication, repair and recombination, DNA in most eukaryotes exists in the form of chromatin; a complex of DNA with nuclear histone proteins that displays multiple levels of folding and compaction<sup>1</sup>. The first level of chromatin organisation is the linear array of nucleosome core particles (NCPs) composed of 145–147 bp DNA wrapped around the histone octamer (HO) core, which is formed by two copies each of the four histones, H2A, H2B, H3, and H4. The NCPs are connected by linker DNA with a variable length in the range 10–80 bp. *In vitro*, the nucleosome arrays appear as extended 10 nm beads-on-a-string fibres at low (few millimolar Na- or KCl) salt solutions, which further fold into the 30-nm fibre upon increase of salt or addition of multivalent cations. The structure of the 30-nm fibre is linker-DNA-length dependent<sup>2</sup> and is a matter of much debate<sup>2,3</sup> and controversy with respect to its relevance *in vivo*<sup>3,4</sup>. Nucleosome arrays further fold into higher order structures by fibre-fibre interactions.

The major component of chromatin, DNA, is negatively charged and DNA-DNA electrostatic repulsion is the primary obstacle for its compaction. Positively charged histones neutralize about 50% of the DNA charge in the NCP. In the histones, a majority of the charge is located in the unstructured flexible N-termini (the histone tails) which protrude outside the NCP and interact with the DNA of its own and neighbouring NCPs, with linker DNA and with other components of chromatin. In higher organisms, an additional class of proteins, the linker histones H1<sup>5</sup> neutralise about half of the charge on the linker DNA. The linker histones contributes to the chromatin structure stabilization and facilitates fibre folding and self-association<sup>6</sup>. However, the viability of the cells is tolerant to depletion of H1 and lower eukaryotes (e.g. yeast) show little change in transcription profile and phenotype after complete knockout of the linker histone<sup>5</sup>. The influence of the amount of histone H1 on nucleosome repeat length (NRL) is well-described by a simple electrostatic mechanism<sup>5,7</sup>. It has been observed that for chromatin with longer NRLs, the maximal folding of the fibres *in vitro* requires linker histones, whereas arrays with shorter NRL (187 bp DNA or less) can reach “native” compaction at millimolar  $Mg^{2+}$  concentrations without histone H1 (see e.g. Refs. 2, 5, 8, 9). The above observations justify the study of model nucleosome arrays lacking linker histones being highly relevant to the *in vivo* situation.

Due to the DNA:histone (1 : 0.5) charge stoichiometry, chromatin can be considered as a polyanion-polycation complex with excessive negative charge but with a population of grafted flexible positively charged chains



(the histone tails) contributing to the chromatin structure and dynamics<sup>10,11</sup>. The polyelectrolyte nature of chromatin is demonstrated by a high sensitivity of its properties to the ionic environment and has recently been studied using well defined *in vitro* systems of nucleosome arrays, self-assembled from recombinant histones and DNA array templates<sup>9,10,12</sup>. A strong dependence of nucleosome array folding and self-association on charge and concentrations of the cations in solution has been demonstrated<sup>12–14</sup>. A sensitivity of chromatin properties to the number, density, and modifications of charged amino acids in the histone tails has been found<sup>15–18</sup>. Generally, an increase of monovalent salt or the addition of multivalent cations increase the compaction of chromatin, switching nucleosome-nucleosome and DNA-DNA interactions from repulsive to attractive by screening DNA charge, increasing DNA flexibility (reducing electrostatic component of the persistence length)<sup>14</sup>, by cation-cation and histone tail-tail correlations and histone tail bridging<sup>10,12,19</sup>.

The vast majority of studies investigating the ionic dependencies of folding and self-association of nucleosome arrays were performed by varying the concentration of a single ionic species, either Na<sup>+</sup> or Mg<sup>2+</sup>. Investigations of the influence of cations other than Na<sup>+</sup> or Mg<sup>2+</sup> (e.g. K<sup>+</sup>, Ca<sup>2+</sup>, or cations with charge higher than +2 like ubiquitous polyamines spermidine<sup>3+</sup> or spermine<sup>4+</sup>) are rare<sup>12,13,20–22</sup>. There exist a few exceptions (e.g. Ref. 23) when *in vivo* relevant conditions of mixtures of cations of different charge (like Na<sup>+</sup> and Mg<sup>2+</sup>) was studied. Widom<sup>21</sup> studied folding and self-association of chromatin fibres, which included a careful analysis (by electron microscopy, small angle X-ray scattering and AUC sedimentation velocity measurements) of fibre properties in mixed NaCl + MgCl<sub>2</sub> solutions. At concentration above 45 mM it was found that Na<sup>+</sup> caused fibre folding but at lower concentrations Na<sup>+</sup> competed with multivalent species (Mg<sup>2+</sup> and trivalent Co(NH<sub>3</sub>)<sub>6</sub><sup>3+</sup>) for binding to the fibre, thus reducing the folding. Oligomerization of the arrays was observed at submillimolar and millimolar concentrations of Mg<sup>2+</sup> both in the absence and in the presence of NaCl and it was also noted that the arrays have a tendency to self-associate when folding to the 30-nm fibre is still incomplete. Similar conclusions about competition between Na<sup>+</sup> and Mg<sup>2+</sup> for binding to the array was made by Borochoy et al observing self-association of chromatin fibres<sup>24</sup>. These results were interpreted<sup>21,25</sup> considering chromatin as a cation-exchange polyelectrolyte, using the Manning counterion condensation model to predict that more Mg<sup>2+</sup> is required to fold or to aggregate chromatin fibre with increase of monovalent salt. However, another study<sup>20</sup> using similar chromatin fibres and ionic concentrations came to the opposite conclusion, namely that the simultaneous presence of Na<sup>+</sup> and Mg<sup>2+</sup> (or Co(NH<sub>3</sub>)<sub>6</sub><sup>3+</sup>) makes a synergistic influence on the fibre self-association; more added Na<sup>+</sup> requires less Mg<sup>2+</sup> (or Co(NH<sub>3</sub>)<sub>6</sub><sup>3+</sup>) to precipitate the fibre. To the best of our knowledge these discrepancies were not later addressed, scrutinised and resolved. The cited works<sup>20,21,24</sup> were performed using fibres extracted by limited micrococcal nuclease digestion of chromatin from chicken erythrocytes that were inhomogeneous with respect to number of nucleosomes, nucleosome repeat length, amount of linker histone H5 and with unknown nature and number of histone posttranslational modifications.

Recently, recombinant model chromatin systems have been developed and after the widespread adoption of the Widom's '601' high-affinity nucleosome positioning sequence<sup>26</sup>, large amounts of highly homogeneous, precisely positioned and fully saturated nucleosome arrays became available. Although this sequence has been generated by artificial selection and do not have natural analogues, the free energy of nucleosome formations for the 601 template is not significantly different from the free energy of nucleosome formation on generic natural DNA sequences. As shown by Widom and co-workers<sup>27</sup>, the free energy of NCP formation differs by about ~4 kcal/mol for DNA sequences with the highest and low-

est known histone octamer binding affinities. It is clear that the differences in free energies of nucleosome formation on different DNA sequences contribute rather marginally to the total free energy of chromatin formation, which is dominated by the huge free energy of (mostly electrostatic) non-specific DNA – histone interaction (tens if not hundreds kcal/mol) and the relatively large cost of the DNA bending (tens of kcal/mol)<sup>11</sup>.

We took advantage of the availability of these pure and well-defined chromatin fibre systems and carried out biophysical studies to gain further understanding of the polyelectrolyte nature of chromatin<sup>12,13</sup>. The purpose of the present work is to determine how folding and self-association of nucleosome arrays proceed when two of the three most common cations of the cell cytoplasm (K<sup>+</sup> + Mg<sup>2+</sup> or Na<sup>+</sup> + Mg<sup>2+</sup>) are simultaneously present. It is generally believed that K<sup>+</sup> and Na<sup>+</sup> have a similar influence on DNA and chromatin and usually this view is supported by observations<sup>28–31</sup> with a few exceptions when the small difference in binding K<sup>+</sup> versus Na<sup>+</sup> is multiplied due to cooperative participation of many DNA charged groups<sup>30</sup> like during the coil-globule transition of high molecular weight DNA<sup>32,33</sup>. Furthermore, we recently found that for 12-mer arrays with nucleosome repeat length of 177 bp (12-177-601 array), potassium prevents complete folding of the arrays at a level almost equal to the strong effect caused by the H4 histone Lys16 acetylation (H4-K16Ac)<sup>22</sup>.

## Results and Discussion

**Nucleosome array folding in mixed-salt solutions.** Folding of the 12-177-601 array is well-characterised in a number of works<sup>9,12,22,34–36</sup>. Analytical ultracentrifugation sedimentation velocity (AUC-SV) measurements show that the array adopts an extended 'beads-on-a-string' conformation with a sedimentation velocity coefficient value,  $s_{20,w}$ , in the range 34–36 S at low salt concentration such as TEK buffer (10 mM Tris·HCl, pH 7.5, 10 mM KCl, 0.1 mM EDTA) used in this work as background in all AUC-SV measurements. Complete folding of the array induced by addition of Na<sup>+</sup> (100 mM), Mg<sup>2+</sup> (1.0 mM) or micromolar concentrations of multivalent cations<sup>12,22</sup> produces compact globular particles<sup>36</sup> with  $s_{20,w}$  values 52–56 S<sup>12,22,34–36</sup>. However, most data in the literature is limited to determination of  $s_{20,w}$  values varying either NaCl or MgCl<sub>2</sub> salt. Some work was done to study the array folding in the presence of other cations<sup>12,22</sup>. We are not aware of data on the folding and self-association of well-defined recombinant arrays in mixtures of the cations K<sup>+</sup>, Mg<sup>2+</sup>, and Na<sup>+</sup>.

Two series of the AUC-SV measurements were carried out for each of the cations, K<sup>+</sup> and Na<sup>+</sup>: In the first series, varying concentrations of Mg<sup>2+</sup> ( $C_{Mg}$ ) was added to an array solution at fixed concentration of KCl (75 and 100 mM) or NaCl (40 and 100 mM). The criterion for the choice of the intermediate (between 0 and 100 mM of added monovalent cation) concentration of either KCl or NaCl was to choose a concentration when the array is moderately folded (that it has an  $s_{20,w}$  value about 45 S) so that both a positive or a negative effect of addition of Mg<sup>2+</sup> can be registered. Since Na<sup>+</sup> induces formation of the 30-nm fibre more efficiently than K<sup>+</sup>, a lower concentration of added Na<sup>+</sup> is required to get this intermediate  $s_{20,w}$  value (40 mM Na<sup>+</sup> versus 75 mM of added K<sup>+</sup>). In Fig. 1, examples of van Holde Weischet curves for the first series of experiments are shown at fixed concentrations of KCl or NaCl with variation of  $C_{Mg}$ . Fig. 2A summarises the results obtained from repeated series of such measurements as illustrated in Fig. 1. The data are represented as the characteristic mean  $s_{20,w}$  value calculated as the mean of the average  $s_{20,w}$  values obtained from 20–80% of the boundary in two to three independent AUC-SV experiments for each condition.

As seen from the boundary curves in Fig. 1, the bulk of the data (except the high-salt mixtures, 100 mM K<sup>+</sup> or Na<sup>+</sup> plus 0.8 or 1.2 mM of Mg<sup>2+</sup>) showed good homogeneity of the array within

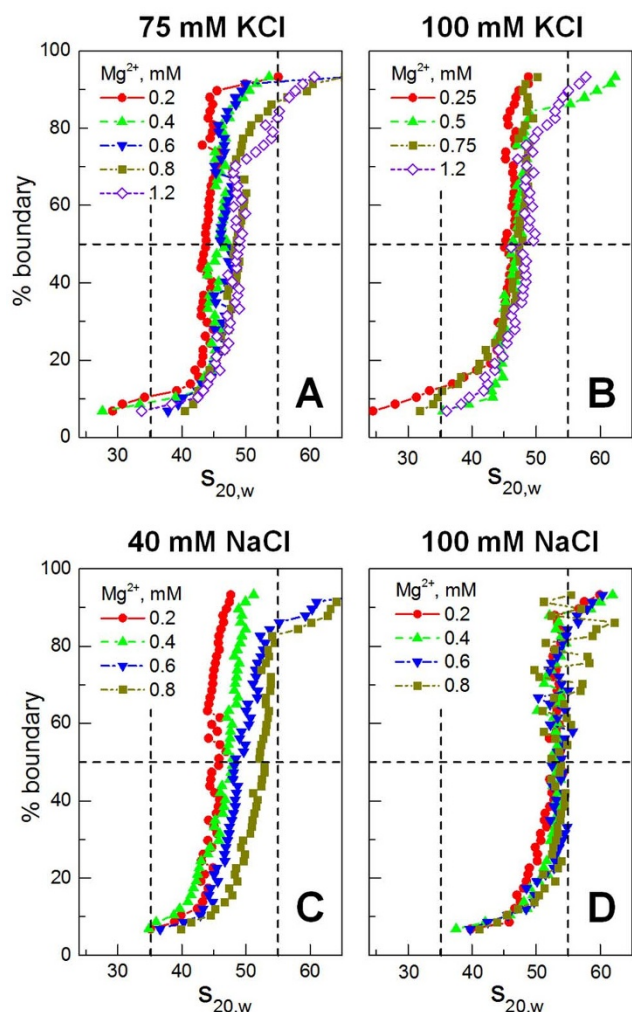


**Figure 1** | van Holde-Weischet analysis of the AUC-SV data obtained in mixed salt solutions. Each graph presents the data determined at fixed concentration of NaCl or KCl (indicated at the top of the graph); each curve in the graphs was recorded for a given  $Mg^{2+}$  concentration. In each graph, the two vertical dashed lines indicate the  $s_{20,w}$  values characteristic of the 12-177-601 array respectively in unfolded state at low salt concentration (TEK buffer;  $s_{20,w} = 35.2$  S) and in fully folded state obtained at 100 mM NaCl ( $s_{20,w} = 55$  S); the horizontal dashed line marks the 50% boundary.

20–80% of the boundary. At 75 mM KCl or 40 mM NaCl, the increase of  $C_{Mg}$  results in further folding of the array (the effect is less pronounced in  $K^+$ , see the curves with hollow symbols in Fig. 2A). On the other hand, at 100 mM KCl or at 100 mM NaCl, the addition of  $Mg^{2+}$  does not significantly increase the array folding (filled circles or filled diamonds in Fig. 2A). At 100 mM KCl plus 0.8 mM  $Mg^{2+}$ , the array is homogenous. However; at 100 mM NaCl with 0.8 mM  $Mg^{2+}$ , the AUC-SV data show dispersion that indicates onset of aggregation (self-association) as seen in Fig. 1D (square symbols). Notably, the characteristic  $s_{20,w}$  values are different in the presence of 100 mM of added KCl or NaCl and are only weakly sensitive to the concentration of added  $Mg^{2+}$ . The  $s_{20,w}$  values are in the range 45–47 S at 100 mM KCl (array is moderately folded); whereas at 100 mM NaCl,  $s_{20,w} \approx 53$ –57 S, indicating complete folding of the fibre (Fig. 1B and D and Fig. 2A). In other words, at higher concentrations relevant to physiological conditions,  $K^+$  and  $Na^+$  exert different influence on the array compaction. The presence of  $K^+$  inhibits the complete array folding and in 75 and 100 mM KCl the  $s_{20,w}$  values are in the range 46–48 S while in the presence of

100 mM NaCl or for solutions of NaCl +  $MgCl_2$ , the array can reach complete compaction with  $s_{20,w} \approx 52$ –56 S.

In the second series of experiments, the AUC-SV measurements were carried out at fixed concentration of  $MgCl_2$  (1 mM) which means the arrays are fully compacted, increasing the concentration of KCl or NaCl (van Holde Weischet curves are not shown). Figure 2B summarises the results of the AUC-SV measurements. It may be noted the data in Fig. 2 from the two series of titrations (varying  $Mg^{2+}$  at fixed KCl/NaCl; fixed  $Mg^{2+}$ , varied KCl/NaCl) obtained in the present study are combined with  $s_{20,w}$  values determined earlier for the same array in solutions with only one added salt ( $MgCl_2$ , KCl, or NaCl)<sup>22</sup>. Addition of KCl or NaCl to low-salt TEK buffer array solution leads to array folding.

The “destructive” effect of  $K^+$  on fibre folding is clearly illustrated by the decrease of the  $s_{20,w}$  values observed upon addition of KCl to the array solution in the presence of 1 mM  $Mg^{2+}$  (Fig. 2B, solid green rhombi). At 1 mM  $Mg^{2+}$ , the fully compacted array “opens up” when  $K^+$  increases. In contrast to  $K^+$ , addition of  $Na^+$  to array solution with 1 mM  $Mg^{2+}$  leads to aggregation (Fig. 2B, solid orange triangles) and the AUC-SV data loses reproducibility which is reflected by loss of homogeneity (large error bars in Fig. 2) and by the fact that  $s_{20,w}$  rises above the values possible for the maximally compacted array (Fig. 2B, data for 1 mM  $Mg^{2+}$  +  $Na^+$  are solid orange triangles). Solutions of the array with  $K^+$  generally show higher homogeneity and AUC-SV curves are reproducible in a wider concentration range compared to the results in NaCl.

The present work confirms our earlier result<sup>12,22</sup> that  $K^+$  prevents complete folding of the array and shows that this unfolding effect of  $K^+$  cannot be overcome by addition of  $Mg^{2+}$ , which is expected to be much more powerful than monovalent cations in screening DNA-DNA repulsion and promoting chromatin compaction. In earlier work, we also found<sup>22</sup> that addition of KCl made a similar inhibitory effect on the array folding as H4 Lys16 acetylation, which is known as the most powerful modification that profoundly abrogates chromatin folding<sup>22,34,37</sup>. Combining experimental data on folding of the different 12-177-601 arrays (in the wild type form, with H4-K16 acetylation or mutation to glutamine), with data on NCP crystal structures saturated with rubidium or caesium salt<sup>38</sup>, this unfolding influence of  $K^+$  (which is also displayed in the presence of  $Rb^+$  or  $Cs^+$ ) led to the suggestion of a novel hypothesis of the structure of the NCP-NCP stacking. In this model, NCP stacking is stabilized by hydrogen bonds between the charged  $\epsilon$ -amino group of the H4-Lys16 and oxygen atoms of the peptide carbonyl in the H2B Arg96-Leu99 pocket<sup>22</sup>. This crucial contact can be disrupted either by H4-K16 acetylation or by coordination of  $K^+$  (or similar  $Rb^+$  and  $Cs^+$ ) with the H2B Arg96-Leu99 pocket. The specific affinity of  $K^+$  (or  $Rb^+$  and  $Cs^+$ ) for the oxygen of peptide carbonyl (as compared to  $Na^+$ ) has been experimentally observed<sup>30</sup>.

It follows from our work that in the cell nucleus, where  $K^+$  is the major cation, the specific tightest NCP-NCP stacking might be inhibited despite the presence of  $Mg^{2+}$ . It would be interesting to investigate if this unfolding effect of  $K^+$  is observed for arrays with different nucleosome repeat length and if other factors (e.g. presence of linker histones), can recover H4-histone-tail-mediated NCP stacking even in the presence of  $K^+$ .

#### Self-association of 12-177-601 arrays in mixed-salt solutions.

Monovalent cations cannot induce self-association of the wild type 12-177-601 array<sup>13,22</sup> whereas addition of divalent  $Mg^{2+}$  leads to complete precipitation.  $Mg^{2+}$ -induced precipitation assay is widely-used to assess the balance of repulsive and attractive interactions in self-association of chromatin fibres as a function of a variety of factors such as nucleosome repeat length<sup>9,36</sup> or modifications in the histone tails<sup>17,18,22,35</sup>.

To test whether monovalent ions affect the efficiency of the  $Mg^{2+}$ -induce inter-array aggregation, a series of  $Mg^{2+}$  titrations were car-



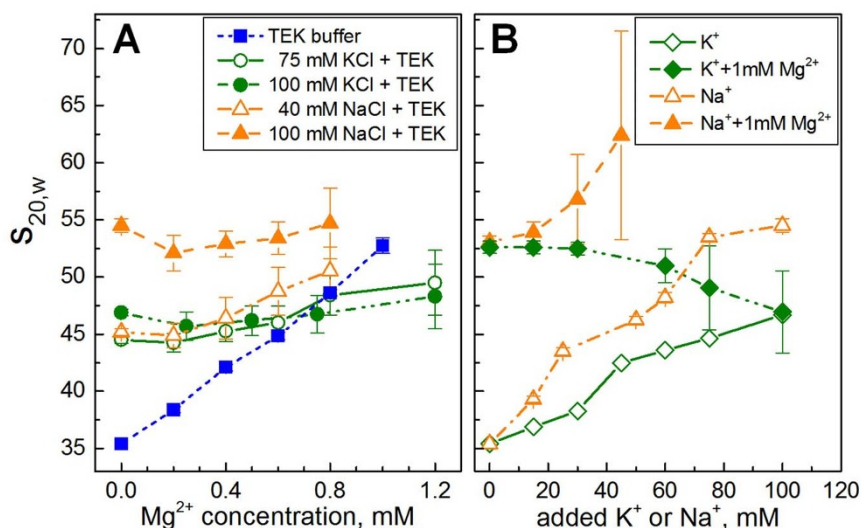


**Figure 2 | Summary of AUC-SV results.** (A). Values of sedimentation velocity coefficient,  $s_{20,w}$ , are displayed as a function of  $Mg^{2+}$  concentration at fixed concentration of added KCl (green) or NaCl (orange). Blue points are  $Mg^{2+}$ -concentration dependence in the absence of added monovalent salt (data from Ref. 22). (B). Dependence of the  $s_{20,w}$  values on KCl or NaCl concentration in the absence of  $Mg^{2+}$  (hollow points; data from Ref. 22) or in the presence of 1 mM  $Mg^{2+}$  (solid points). All solutions contained TEK buffer. Error bars were calculated from 2–3 independent AUC scans and using  $s_{20,w}$  values within 20–80% of boundary. For 1 mM  $Mg^{2+}$  with added NaCl (solid triangles in (B)), the  $s_{20,w}$  values exceed the ones expected for the fully folded array ( $\sim 55$  S) and are of low quality (as indicated by large error bars) demonstrating array aggregation.

ried out in 10 mM Tris·HCl, pH 7.5 buffer containing a fixed concentration of the monovalent salt. The concentration of the array used in the precipitation assay was similar to the one used in the AUC-SV measurements ( $A^{259} = 0.8$ – $1.0$ ). Figure 3 displays precipitation curves of the arrays in solutions with KCl (Fig. 3A) or NaCl (Fig. 3B). Increase in  $K^+$  or  $Na^+$  leads to decrease of the  $Mg^{2+}$  concentration required to induce array precipitation. Figure 4 shows  $EC_{50}$  values (the  $Mg^{2+}$  concentrations that induce 50% precipitation of the array) determined in mixed salt solution compared with the  $EC_{50}$  values found in titration without added salt. Addition of KCl or NaCl produces a similar effect on the  $EC_{50}$  values: less  $Mg^{2+}$  is required to precipitate the array. The precipitation assay curves (Fig. 3) in the presence of KCl and NaCl are rather broad and some array aggregation is observed already at 1 mM  $Mg^{2+}$ . It is plausible that this fraction of aggregated arrays makes an influence on the AUC measurements causing broadening of the van Holde-Weischet curves (Fig. 1) and larger error bars (Fig. 2).

In the presence of 100 mM salt, the  $EC_{50}$  values are close to 1 mM, which explains why aggregation of the arrays limits application of the AUC-SV method in mixed solution at high monovalent salt. Array precipitation by  $Mg^{2+}$  occurs in a quite broad range of added  $Mg^{2+}$  (Fig. 3) and one needs to be cautious in interpretation of the  $EC_{50}$  data. However, the  $EC_{50}$  values in the presence of NaCl salt are typically lower than the corresponding ones determined in KCl. The somewhat higher efficiency of  $Na^+$  ions relative to  $K^+$  might originate from preferential binding of  $Na^+$  (relative to  $K^+$ ) to the phosphate groups of DNA<sup>39</sup> and to the carboxylic groups<sup>40</sup> (important for screening the H2A acidic patch on the HO surface)<sup>22</sup>. These specific interactions can increase quenching of the negative charge of the array and facilitate its self-association.

**Conclusions.** Both nucleosome array folding and self-association are determined by electrostatic interactions with the repulsion between the negatively charged DNA as the major force that drives the formation of an extended “beads-on-a-string” structure at low monovalent salt concentrations, while the nature of the cation is of minor importance.

In the folded/aggregated state, the detailed molecular structure of the chromatin and the interplay between intra- (formation of the

folded 30-nm fiber) and inter-array condensation is dependent on the DNA molecular structure and sequence, NRL, the histones, as well as nature and amount of salt cations. E.g., the NRL will profoundly influence the ability of folding in the absence of linker histone<sup>2,9,36</sup>. The most important structural element of maximally folded chromatin is the NCP-NCP stacking and *in vitro* and *in vivo* studies indicate that there exists multiple nucleosome stacking conformations. A major conclusion from Fig. 2 is that for the 12-177-601 array, the  $K^+$  and  $Na^+$  ions have a different influence on the array folding, especially at physiologically relevant  $K^+/Na^+$  and  $Mg^{2+}$  concentrations; one ion ( $Na^+$ ) promotes stacking while the other ( $K^+$ ) abrogates it.

We may question how relevant the findings of the present study are to the situation *in vivo*? We argue that the range of  $K^+$ ,  $Na^+$  and  $Mg^{2+}$  activities applied in the AUC-SV and PA studies are in the range of ionic activities of the eukaryotic cell cytoplasm. To support this claim we would like to note that low molecular weight species (with molecular mass below 50 kDa) can freely exchange between the nucleus and cytoplasm through nuclear pores and as a consequence the small and highly mobile cations  $K^+$ ,  $Mg^{2+}$ ,  $Na^+$  and  $Ca^{2+}$  are in thermodynamic equilibrium within the entire cell. Therefore, *activities* of these cations are equal in the cytoplasm and in the nucleoplasm but their *amounts and concentrations* in various cell organelles with significant binding to the biomolecules, are expected to be very different. This reflects the variable amount and different cation affinities of the anionic groups present in the given organelle or biomolecule. E.g., the average concentration over the whole cell volume is estimated at 7–9 mM for  $Ca^{2+}$  in interphase cells<sup>41</sup>. However, the activity or concentration of “free”  $Ca^{2+}$  is strictly regulated and maintained at micromolar levels by the presence of a large amount of Ca-selective proteins (e.g. calmodulin). The contribution of  $Ca^{2+}$  to chromatin properties is therefore expected to be insignificant, since the  $Ca^{2+}$  affinity to DNA is negligible in comparison to the binding constants of the specialized proteins. Data on the amount or total concentration of  $K^+$ ,  $Na^+$ ,  $Mg^{2+}$  inside the eukaryotic cell and its compartments varies significantly. As reported<sup>41</sup>, the local concentration (not activity) of  $Mg^{2+}$  vary in the range 2–32 mM depending on the cell type, cell cycle and cell organelle. In a relevant book<sup>42</sup>, the concentration of “free”  $Mg^{2+}$  in

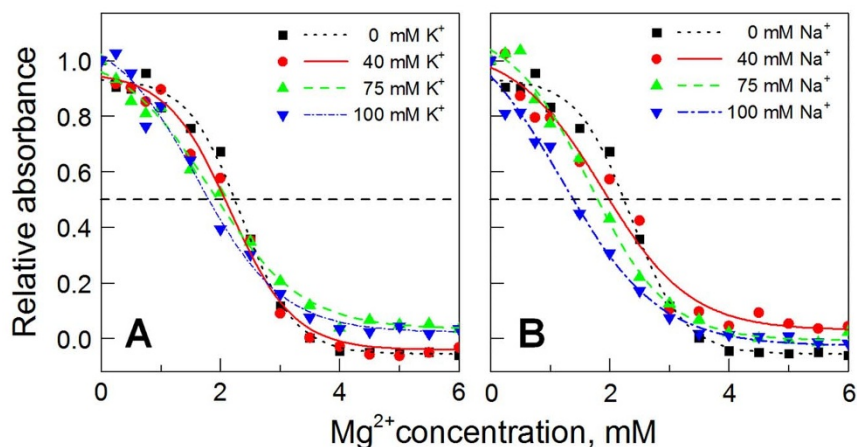


**Figure 3** |  $Mg^{2+}$ -induced precipitation of the nucleosome arrays. Relative absorbance at 259 nm determined in the supernatant of the array solution with fixed concentrations of KCl (A) or NaCl (B) is plotted as a function of  $MgCl_2$  concentration. (All solutions contained 10 mM Tris buffer, pH 7.5). Points are experimental results; curves are sigmoidal fitting of the data. The dashed horizontal line indicates the midpoint of precipitation ( $EC_{50}$ ).

the cell is estimated at about 0.5 mM, while the “total” concentration might be as high as 40 mM<sup>43</sup>. Regarding average concentrations of  $K^+$  and  $Na^+$ , X-ray microanalysis<sup>41</sup> does not report absolute values, but give data for the  $K^+$  enrichment in the nucleus. The distinction between the ionic concentration and ion activity of  $K^+$  and  $Na^+$  in the cytoplasm is rarely acknowledged and reported. In a relevant paper<sup>44</sup>, the concentrations and activities of  $K^+$ ,  $Na^+$  and  $Cl^-$  in Ehrlich ascites tumor cells were measured and the following concentration/activity values were obtained:  $Na^+$ : 25.3/4.6 mM;  $K^+$ : 165.1/68.3 mM;  $Cl^-$ : 65.3/43.6 mM. The observations and arguments presented above justifies the relevance of our experimental setup that obviously simplifies the situation *in vivo*, but nevertheless exhibits an essential feature: the mixing of monovalent  $K^+$  or  $Na^+$  (at concentrations of 100 mM or below) with  $Mg^{2+}$  at millimolar concentrations is physiologically relevant. An important conclusion is that one needs to be cautious in extrapolation of results of *in vitro* studies of chromatin routinely carried out in sodium salts to the *in vivo* conditions where potassium cations are dominant.

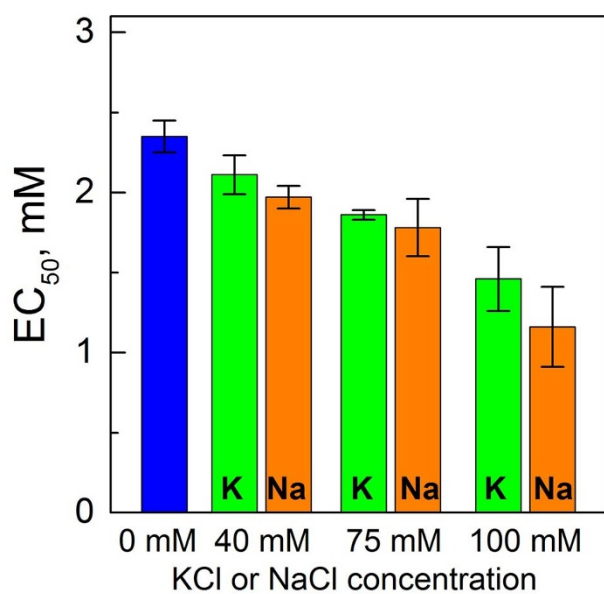


**Figure 4** | Summary of the precipitation assay results. Midpoints of the  $Mg^{2+}$ -induced precipitation,  $EC_{50}$ , obtained in 10 mM Tris·HCl, pH 7.5 buffer without added monovalent salt (blue bar) or with 40, 75, 100 mM of added KCl (green) or NaCl (orange).

## Methods

**Histone and DNA preparation.** The DNA template containing the 12 tandem 177 bp repeats of the high-affinity Widom '601<sup>26</sup> nucleosome positioning sequence (abbreviated as 12-177-601) was used. The pWM530 plasmid vector carrying 12-177-601 sequence was transformed to *E.coli* HB101 competent cell and amplified and purified as described previously<sup>35</sup>. *Xenopus laevis* histones H2A, H2B, H3, and H4 were individually expressed in *E.coli* BL21 DE3 PlyS and purified using ÄKTA FPLC system (Uppsala, Sweden) in two stages: by gel filtration on Sephacryl S200 column followed by cation exchange chromatography using Resource S column<sup>45</sup>. Histone octamer (HO) was refolded using 1 : 1.2 : 1.2 molar ratio for the H2A, H2B, H3, and H4 respectively. The HO was purified on Superdex M 200 column (ÄKTA FPLC system)<sup>45</sup>.

**Nucleosome array preparation.** Nucleosome 12-177-601 arrays were prepared from the recombinant the 12-177-601 DNA template and the histones as described previously<sup>12</sup>. Briefly, small-scale nucleosome array reconstruction trials were carried out to determine an optimal HO:DNA stoichiometry. The optimal HO:DNA ratio (12.5 moles of HO per one mole of 12-177-601 DNA) was used for large scale array preparation. It included step-wise dialysis of the mixture of HO, 12-177-601 DNA, and competitor 145 bp DNA from 2 M KCl to TEK buffer (10 mM Tris·HCl pH 7.5, 10 mM KCl, 0.1 mM EDTA) followed by purification by  $MgCl_2$  precipitation and redissolution in TEK buffer as described previously<sup>12,36</sup>. The competitor DNA was obtained from nuclease-digested calf thymus chromatin and was about 145 bp length. The concentration of competitor DNA was 0.6 fragments per one molecule of 12-177-601 DNA. The reconstituted arrays were digested by ScaI (a ScaI restriction site is at linker DNA of each of the 12 repeats) and analysed by 6% native polyacrylamide gel electrophoresis (PAGE) to check saturation of the array with HO (see for details)<sup>12,36</sup>.

Stock solution of the 12-177-601 array (~2 mg/mL in TEK buffer) was stored at 4°C and used in AUC and precipitation assay experiments. The quality of array was checked upon reconstitution and after one-two week storage by: a) running both native array and ScaI digested on 0.8% agarose and 6% DNA-PAGE gel to assess the purity and saturation (via measuring of free 177 DNA formation after digestion with ScaI). b) Running AUC-VC measurement at 1 mM  $MgCl_2$ . Absence of the 177 bp lane in the ScaI-digested array and an  $s_{20,w}$  value of 52–53 S indicates a homogeneous and saturated sample. Since this study compares the effect of KCl and NaCl, it may be asked whether the reconstitution nature of the salt influence the properties of resulting stock solution. In our laboratory, fibres were reconstituted in KCl<sup>12,22</sup>. In the Richmond group<sup>35</sup>, the 12-177-601 arrays fibres were reconstituted in NaCl using the same source of DNA and histones. Identical results were obtained for the  $Mg^{2+}$ -induced compaction, which shows that reconstitution in potassium or sodium environments, results in fibres with identical folding properties.

**Analytical Ultracentrifugation (AUC).** Analytical ultracentrifugation sedimentation velocity (AUC-SV) method provides information about degree of folding of nucleosome arrays and regularly used in studies of chromatin<sup>16,46</sup>. AUC-SV measurements were carried out using a Beckman XL-A/XL-I analytical ultracentrifuge (Beckman Coulter, Fullerton, CA). The nucleosome arrays were diluted in TEK buffer to optical density  $A_{259} = 0.8 \text{ cm}^{-1}$ . Samples and references were equilibrated in 12 mm double-sector cells under vacuum, for 30 min at 20°C and at 3000 rpm. Forty scans were collected at 12,000 rpm with 10 min interval. The data was analysed using the van Holde Weischet method<sup>47</sup> by the UltrascanII program<sup>48</sup> and plotted as integrated curves of boundary versus sedimentation coefficient (Fig. 1). The sedimentation velocity coefficient was corrected to  $s_{20,w}$  using a partial specific volume of 0.622 mL/g<sup>35</sup>. For each AUC-SV measurement, characteristic mean  $s_{20,w}$



value was calculated as the average of  $s_{20,w}$  from 20–80% of the boundary, each characterized by a given standard deviation. Two–three independent AUC–SV runs were performed for each array sample and the mean  $s_{20,w}$  value was calculated from the average  $s_{20,w}$  (obtained from 20–80% of the boundary) with the standard deviation (SD) obtained as the root mean square of the corresponding SDs.

**Precipitation assay (PA).** The stock solution of the array was diluted in 10 mM Tris–HCl, pH 7.5 to optical density  $A^{259} = 2$  after which the solution was mixed with equal volume of the same buffer containing twice the final concentration of mono- and divalent salt. The absorbance of the final solution was  $A^{259} = 1$ , similar to the one used in the AUC–SV method. After incubation for 15 min, the samples were spun for 15 min  $\times$  20,000 g at room temperature. The absorbance of the supernatant was measured at 259 nm using NanoDrop ND-1000 UV/Vis spectrophotometer (NanoDrop Technologies, Wilmington, DE); the range of  $A^{259}$  absorbance used in the PA corresponds to the best precision of the spectrophotometric measurements. The efficiency of mixed cation system to precipitate the array was characterized by the average  $Mg^{2+}$  concentration at 50% precipitation of the array ( $EC_{50}$ ) calculated from at least three measurements.

- Wolffe, A. P. *Chromatin: Structure and function*, 447 (Academic Press, San Diego, CA, 1998).
- Routh, A., Sandin, S. & Rhodes, D. Nucleosome repeat length and linker histone stoichiometry determine chromatin fiber structure. *Proc. Natl. Acad. Sci. U. S. A.* **105**, 8872–8877 (2008).
- Grigoryev, S. A. & Woodcock, C. L. Chromatin organization - The 30 nm fiber. *Exp Cell Res.* **318**, 1448–1455 (2012).
- Maeshima, K., Imai, R., Tamura, S. & Nozaki, T. Chromatin as dynamic 10-nm fibers. *Chromosoma* **123**, 225–237 (2014).
- Woodcock, C. L., Skultchi, A. I. & Fan, Y. Role of linker histone in chromatin structure and function: H1 stoichiometry and nucleosome repeat length. *Chromosome Res.* **14**, 17–25 (2006).
- Carruthers, L. M., Bednar, J., Woodcock, C. L. & Hansen, J. C. Linker histones stabilize the intrinsic salt-dependent folding of nucleosomal arrays: mechanistic ramifications for higher-order chromatin folding. *Biochemistry* **37**, 14776–14787 (1998).
- Blank, T. A. & Becker, P. B. Electrostatic mechanism of nucleosome spacing. *J. Mol. Biol.* **252**, 305–313 (1995).
- Robinson, P. J. J., Fairall, L., Hlynh, V. A. T. & Rhodes, D. EM measurements define the dimensions of the “30-nm” chromatin fiber: Evidence for a compact, interdigitated structure. *Proc. Natl. Acad. Sci. U. S. A.* **103**, 6506–6511 (2006).
- Correll, S. J., Schubert, M. H. & Grigoryev, S. A. Short nucleosome repeats impose rotational modulations on chromatin fibre folding. *EMBO J.* **31**, 2416–2426 (2012).
- Korolev, N., Allahverdi, A., Lyubartsev, A. P. & Nordenskiöld, L. The polyelectrolyte properties of chromatin. *Soft Matter* **8**, 9322–9333 (2012).
- Korolev, N., Vorontsova, O. V. & Nordenskiöld, L. Physicochemical analysis of electrostatic foundation for DNA–protein interactions in chromatin transformations. *Prog. Biophys. Mol. Biol.* **95**, 23–49 (2007).
- Korolev, N. *et al.* Electrostatic origin of salt-induced nucleosome array compaction. *Biophys. J.* **99**, 1896–1905 (2010).
- Korolev, N. *et al.* The effect of salt on oligocation-induced chromatin condensation. *Biochem. Biophys. Res. Comm.* **418**, 205–210 (2012).
- Carrivain, P. *et al.* Electrostatics of DNA compaction in viruses, bacteria and eukaryotes: functional insights and evolutionary perspective. *Soft Matter* **8**, 9285–9301 (2012).
- Woodcock, C. L. & Dimitrov, S. Higher-order structure of chromatin and chromosomes. *Curr. Opin. Genet. Dev.* **11**, 130–135 (2001).
- Hansen, J. C. Conformational dynamics of the chromatin fiber in solution: determinants, mechanisms, and functions. *Annu. Rev. Biophys. Biomol. Struct.* **31**, 361–392 (2002).
- Kan, P.-Y., Lu, X., Hansen, J. C. & Hayes, J. J. The H3 tail domain participates in multiple interactions during folding and self-association of nucleosome arrays. *Mol. Cell. Biol.* **27**, 2084–2091 (2007).
- McBryant, S. J. *et al.* Determinants of histone H4 N-terminal domain function during nucleosomal array oligomerization: roles of amino acid sequence, domain length, and charge density. *J. Biol. Chem.* **284**, 16716–16722 (2009).
- Korolev, N., Fan, Y., Lyubartsev, A. P. & Nordenskiöld, L. Modelling chromatin structure and dynamics: status and prospects. *Curr. Opin. Struct. Biol.* **22**, 151–159 (2012).
- Sen, D. & Crothers, D. M. Condensation of chromatin: Role of multivalent cations. *Biochemistry* **25**, 1495–1503 (1986).
- Widom, J. Physicochemical studies of the folding of the 100 A nucleosome filament into the 300 A filament. Cation dependence. *J. Mol. Biol.* **190**, 411–424 (1986).
- Allahverdi, A. *et al.* The effects of histone H4 tail acetylations on cation-induced chromatin folding and self-association. *Nucleic Acids Res.* **39**, 1680–1691 (2011).
- Kruthof, M. *et al.* Single-molecule force spectroscopy reveals a highly compliant helical folding for the 30-nm chromatin fiber. *Nat. Struct. Mol. Biol.* **16**, 534–540 (2009).
- Borochof, N., Ausio, J. & Eisenberg, H. Interaction and conformational changes of chromatin with divalent ions. *Nucleic Acids Res.* **12**, 3089–3096 (1984).
- Clark, D. J. & Kimura, T. Electrostatic mechanism of chromatin folding. *J. Mol. Biol.* **211**, 883–896 (1990).
- Lowary, P. T. & Widom, J. New DNA sequence rules for high affinity binding to histone octamer and sequence-directed nucleosome positioning. *J. Mol. Biol.* **276**, 19–42 (1998).
- Thäström, A., Lowary, P. T. & Widom, J. Measurement of histone–DNA interaction free energy in nucleosomes. *Methods* **33**, 33–44 (2004).
- Braunlin, W. H. & Nordenskiöld, L. A potassium-39 NMR study of potassium binding to double-helical DNA. *Eur. J. Biochem.* **142**, 133–137 (1984).
- Korolev, N., Lyubartsev, A. P., Rupprecht, A. & Nordenskiöld, L. Experimental and Monte Carlo simulation studies on the competitive binding of  $Li^+$ ,  $Na^+$ , and  $K^+$  ions to DNA in oriented DNA fibers. *J. Phys. Chem. B* **103**, 9008–9019 (1999).
- Korolev, N. & Nordenskiöld, L. Influence of alkali cation nature on structural transitions and reactions of biopolyelectrolytes. *Biomacromolecules* **1**, 648–655 (2000).
- Korolev, N., Lyubartsev, A. P., Rupprecht, A. & Nordenskiöld, L. Competitive binding of  $Mg^{2+}$ ,  $Ca^{2+}$ ,  $Na^+$ , and  $K^+$  to DNA in oriented DNA fibers: experimental and Monte Carlo simulation results. *Biophys. J.* **77**, 2736–2749 (1999).
- Zinchenko, A. A. & Yoshikawa, K.  $Na^+$  shows a markedly higher potential than  $K^+$  in DNA compaction in a crowded environment. *Biophys. J.* **88**, 4118–4123 (2005).
- Hibino, K. *et al.*  $Na^+$  more strongly inhibits DNA compaction by spermidine ( $3^+$ ) than  $K^+$ . *Chem. Phys. Lett.* **426**, 405–409 (2006).
- Shogren-Knaak, M. A. *et al.* Histone H4–K16 acetylation controls chromatin structure and protein interactions. *Science* **311**, 844–847 (2006).
- Dorigo, B., Schalch, T., Bystricky, K. & Richmond, T. J. Chromatin fiber folding: requirement for the histone H4 N-terminal tail. *J. Mol. Biol.* **327**, 85–96 (2003).
- Schalch, T. The 30-nm chromatin fiber: in vitro reconstitution and structural analysis. Ph. D. Thesis, Swiss Federal Institute of Technology, Zurich (2004).
- Robinson, P. J. J. *et al.* 30 nm chromatin fibre decompaction requires both H4–K16 acetylation and linker histone eviction. *J. Mol. Biol.* **381**, 816–825 (2008).
- Mohideen, K., Muhammad, R. & Davey, C. A. Perturbations in nucleosome structure from heavy metal association. *Nucleic Acids Res.* **38**, 6301–6311 (2010).
- Cheng, Y., Korolev, N. & Nordenskiöld, L. Similarities and differences in interaction of  $K^+$  and  $Na^+$  with condensed ordered DNA. A molecular dynamics simulation study. *Nucleic Acids Res.* **34**, 686–696 (2006).
- Gregor, H. P., Hamilton, M. J., Oza, R. J. & Bernstein, F. Studies on ion exchange resins. XV. Selectivity coefficients of methacrylic acid resins toward alkali metal cations. *J. Phys. Chem.* **60**, 263–267 (1956).
- Strick, R., Strissel, P. L., Gavrillov, K. & Levi-Setti, R. Cation–chromatin binding as shown by ion microscopy is essential for the structural integrity of chromosomes. *J. Cell Biol.* **155**, 899–910 (2001).
- Frausto da Silva, J. J. R. & Williams, R. J. P. *The biological chemistry of the elements. The inorganic chemistry of life*, p. 244–245 (Clarendon Press, Oxford, 1993).
- Collins, K. D. Ion hydration: Implications for cellular function, polyelectrolytes, and protein crystallization. *Biophys. Chem.* **119**, 271–281 (2006).
- Dawson, D. W. & Smith, T. C. Intracellular  $Na^+$ ,  $K^+$  and  $Cl^-$  activities in Erlich ascites tumor cells. *Biochim. Biophys. Acta* **860**, 293–300 (1986).
- Luger, K., Rechsteiner, T. J. & Richmond, T. J. Preparation of nucleosome core particle from recombinant histones. *Methods Enzymol.* **304**, 3–19 (1999).
- Ausio, J. Analytical ultracentrifugation and the characterization of chromatin structure. *Biophys. Chem.* **86**, 141–153 (2000).
- van Holde, K. E. & Weischet, W. O. Boundary analysis of sedimentation-velocity experiments with monodisperse and polydisperse solutes. *Biopolymers* **17**, 1387–1403 (1978).
- Demeler, B. UltraScan. A comprehensive data analysis software package for analytical ultracentrifugation experiments. in *Modern analytical ultracentrifugation: Techniques and methods* (eds. Scott, D. J., Harding, S. E. & Rowe, A. J.) 210–229 (Royal Society of Chemistry, Cambridge, UK, 2005).

## Acknowledgments

We are thankful to Dr. Curt Davey and Prof. Timothy Richmond for gifts of the plasmids encoding DNA and core histones. This work has been supported by the Singapore Agency for Science Technology and Research (A\*STAR) through the Biomedical Research Council grant no. 10/122/19/666 and by the Singapore Ministry of Education Academic Research Fund (AcRF) through a Tier 3 Grant (MOE2012-T3-1-001).

## Author contributions

A.A., N.K. and L.N. design the research. Q.C. and A.A. performed the experiments. A.A., Q.C. and N.K. analysed the results. N.K. and L.N. wrote the paper.

## Additional information

**Competing financial interests:** The authors declare no competing financial interests.

**How to cite this article:** Allahverdi, A., Chen, Q., Korolev, N. & Nordenskiöld, L. Chromatin compaction under mixed salt conditions: Opposite effects of sodium and potassium ions on nucleosome array folding. *Sci. Rep.* **5**, 8512; DOI:10.1038/srep08512 (2015).



This work is licensed under a Creative Commons Attribution-NonCommercial-NoDerivs 4.0 International License. The images or other third party material in this article are included in the article's Creative Commons license, unless indicated otherwise in the credit line; if the material is not included under the Creative

Commons license, users will need to obtain permission from the license holder in order to reproduce the material. To view a copy of this license, visit <http://creativecommons.org/licenses/by-nc-nd/4.0/>